Stem Cell Research 16 (2016) 597–606

Contents lists available at ScienceDirect

Stem Cell Research

journal homepage: www.elsevier.com/locate/scr

CD133 does not enrich for the stem cell activity *in vivo* in adult mouse prostates

Xing Wei [a,b], Arturo V. Orjalo [c], Li Xin [a,d,e,*]

[a] Department of Molecular and Cellular Biology, Baylor College of Medicine, United States
[b] Graduate Program in Integrative Molecular and Biomedical Sciences, Baylor College of Medicine, United States
[c] Biological Technologies, Analytical Development & Quality Control, Genentech Inc., United States
[d] Department of Pathology and Immunology, United States
[e] Dan L. Duncan Cancer Center, Baylor College of Medicine, United States

ARTICLE INFO

Article history:
Received 25 September 2015
Received in revised form 12 February 2016
Accepted 10 March 2016
Available online 11 March 2016

Keywords:
Prostate stem cells
CD133
Lineage tracing

ABSTRACT

CD133 is widely used as a marker for stem/progenitor cells in many organ systems. Previous studies using *in vitro* stem cell assays have suggested that the CD133-expressing prostate basal cells may serve as the putative prostate stem cells. However, the precise localization of the CD133-expressing cells and their contributions to adult murine prostate homeostasis *in vivo* remain undetermined. We show that loss of function of CD133 does not impair murine prostate morphogenesis, homeostasis and regeneration, implying a dispensable role for CD133 in prostate stem cell function. Using a CD133-CreER^{T2} model in conjunction with a fluorescent report line, we show that CD133 is not only expressed in a fraction of prostate basal cells, but also in some luminal cells and stromal cells. CD133^{+} basal cells possess higher *in vitro* sphere-forming activities than CD133^{-} basal cells. However, the *in vivo* lineage tracing study reveals that the two cell populations possess the same regenerative capacity and contribute equally to the maintenance of the basal cell lineage. Similarly, CD133^{+} and CD133^{-} luminal cells are functionally equivalent in maintaining the luminal cell lineage. Collectively, our study demonstrates that CD133 does not enrich for the stem cell activity *in vivo* in adult murine prostate. This study does not contradict previous reports showing CD133^{+} cells as prostate stem cells *in vitro*. Instead, it highlights a substantial impact of biological contexts on cellular behaviors.

1. Introduction

CD133, also known as Prominin-1, is a pentaspan transmembrane glycoprotein (Miraglia et al., 1997) containing two large extracellular and two small intracellular loops. Since its discovery in 1997 (Yin et al., 1997; Weigmann et al., 1997), CD133 has been shown to be widely expressed in many tissues, including kidney (Weigmann et al., 1997), pancreas (Oshima et al., 2007), liver (Kordes et al., 2007; Karbanova et al., 2008), mammary glands (Florek et al., 2005), and prostate (Richardson et al., 2004; Missol-Kolka et al., 2011), *etc.* To this end, only very limited knowledge has been obtained regarding the physiological function of CD133 in development. For examples, loss of CD133 in mice results in defects in disk formation of photoreceptors (Zacchigna et al., 2009) and mutations in CD133 are associated with some human ocular diseases (Maw et al., 2000; Yang et al., 2008; Zhang et al., 2007). Despite a lack of understanding of CD133-mediated biology, it has been shown to serve as a marker for stem cells or progenitors in many organ systems, such as the hematopoietic system (Yin et al., 1997), brain (Weigmann et al., 1997), small intestine (Zhu et al., 2009), muscle (Alessandri et al., 2004), skin (Belicchi et al., 2004), as well as prostate (Richardson et al., 2004; Missol-Kolka et al., 2011).

However, there are some controversial reports. For example, Zhu et al. reported that CD133 is co-expressed with stem cell marker Lgr5 in cells at the base of small intestine crypts and those cells are able to generate the entire small intestinal epithelia (Zhu et al., 2009). But the other study showed that CD133 is expressed in both the Lgr5^{+} intestinal stem cells and the transit-amplifying progenitors (Snippert et al., 2009). In contrast to its role as a stem/progenitor cell marker, Shmelkov et al. reported a ubiquitous expression of CD133 in the differentiated colonic epithelia (Shmelkov et al., 2008). In the human prostate, an $\alpha_2\beta_1^{hi}$/CD133^{+} basal population has been shown to display higher *in vitro* colony-forming ability and was capable of generating prostatic tissues when transplanted subcutaneously in immunodeficient mice (Richardson et al., 2004). A small fraction of human primary prostate epithelial cells expressing CD133 can self-renew and regenerate whole cell populations (Dail et al., 2014). However, Missol-Kolka et al. reported that CD133^{+} cells can be detected in both human and rodent

* Corresponding author at: Baylor College of Medicine, One Baylor Plaza, Houston, TX 77030, United States.
E-mail address: xin@bcm.edu (L. Xin).

http://dx.doi.org/10.1016/j.scr.2016.03.003

prostate luminal cells (Missol-Kolka et al., 2011), indicating that CD133 may not be exclusively expressed in the basal stem cells.

These controversies could be accounted for by the specificity of the CD133 antibodies utilized in different studies. The mature form of CD133 on the plasma membrane is highly glycosylated in the extracellular loops (Miraglia et al., 1997). AC133, which is a glycosylation-dependent epitope of CD133, has been utilized as a cell surface marker to isolate human hematopoietic stem cells (Yin et al., 1997). In the prostate, a rare population of $\alpha_2\beta_1^{hi}$/CD133$^+$ cells was detected in the basal layer of human prostate by the AC133 antibody (Richardson et al., 2004). In contrast, some luminal cells were also shown positive when stained with other antibodies against synthetic CD133 peptides (Missol-Kolka et al., 2011).

In this study, we took advantage of a CD133-CreER^{T2} mouse model that enables the expression of the CreER^{T2} transgene driven by the endogenous CD133 promoter. We examined the localization of CD133-expressing cells in different prostate lineages by breeding the CD133-CreER^{T2} mice with a fluorescent report line. We also employed the model to determine whether CD133-expressing cells function as stem cells *in vivo* by lineage tracing.

2. Materials and methods

2.1. Mice

The CD133-CreER^{T2} mice were purchased from Jackson Laboratory (Bar Harbor, ME). The Rosa26-eYFP mice were obtained from Dr. Andrew Groves at Baylor College of Medicine. Mice were genotyped by polymerase chain reaction (PCR) using mouse genomic DNA from tail biopsy specimens. The sequences of genotyping primers for CreER^{T2} are (forward) 5′-CCTGACAGTGACGGTCCAAAG-3′, and (reverse) 5′-CATGACTCTTCAACTCAAACT-3′. The expected band size for CreER^{T2} PCR is 700 bp. The sequences of genotyping primers for Rosa26-eYFP are (forward) 5′-CTCTGCTGCCTCCTGGCTTCT-3′, (wild-type reverse) 5′-CGAGGCGGATCACAAGCAATA-3′, and (transgene reverse) 5′-TCAA TGGGCGGGGGTCGTT-3′. The expected sizes of PCR products for homozygous, heterozygous, and wild type mice are 250 bp (single band), 250 bp and 330 bp (two bands), and 330 bp (single band), respectively. PCR products were separated electrophoretically on 1% agarose gels and visualized *via* ethidium bromide under UV light.

2.2. Tamoxifen treatment

Tamoxifen (Sigma-Aldrich, St Louis, MO) was dissolved into vegetable oil and was administrated intraperitoneally into experimental mice at the age of 5 weeks (4 mg per 40 g per day for 4 consecutive days).

2.3. Castration and androgen replacement

Experimental mice were castrated at the age of 8 weeks using standard techniques (Valdez et al., 2012). Two weeks after castration, androgen pellets (15 mg/pellet, Sigma-Aldrich, St Louis, MO) were placed subcutaneously to restore serum testosterone level and stimulate prostate regeneration for two weeks. Subsequently, androgen pellets were removed to re-induce prostate regression for two weeks and were replaced to re-induce regeneration for another two weeks.

2.4. RNA in situ hybridization

Adult mice were treated with tamoxifen for 4 consecutive days and sacrificed on the fifth day. Freshly dissected kidney tissues were embedded in O.C.T. Compound (Sakura, Alphen aan den Rijn, Netherlands), and frozen on liquid nitrogen. CD133 and eYFP transcripts were detected in frozen kidney sections by the DesignReady eGFP-Quasar 570 probe set (VSMF-1014-5, Biosearch Technologies, Petaluma, CA), and custom CD133-Quasar 670 probe set (Biosearch Technologies, Petaluma, CA). Sequences for the CD133-Quasar 670 probe set are listed in Supplementary Table 1. The RNA *in situ* hybridization assay was performed as described previously (Facciponte et al., 2014).

2.5. Prostate sphere and prostate organoid assays

Dissociated single prostate cells were prepared as described previously (Valdez et al., 2012). Briefly, prostate tissues were digested in Dulbecco's modified eagle medium (DMEM)/F12/collagenase/hyaluronidase/FBS (StemCell Technologies, Vancouver, Canada) for 3 h at 37 °C, followed by a one-hour digestion in 0.25% Trypsin–EDTA (Invitrogen, Carlsbad, CA) on ice. Subsequently, digested cells were suspended in Dispase (Invitrogen; 5 mg/ml) and DNase I (Roche Applied Science, Indianapolis, IN; 1 mg/ml), and pipetted vigorously to dissociate cell clumps. Dissociated cells were then passed through 70 μm cell strainers (BD Biosciences, San Jose, CA) to get single cells.

The prostate sphere assay was performed as described previously (Xin et al., 2007). Briefly, 1–2 × 10^4 dissociated prostate cells were cultured in 1:1 Matrigel/PrEGM (Matrigel (BD Biosciences, San Jose, CA)/PrEGM (Lonza, Walkersville, MD)). Prostate spheres were defined as spheroids with a diameter >30 μm after a 6-day culture.

The organoid culture was performed following the previous study (Karthaus et al., 2014; Kwon et al., 2015). Briefly, murine prostate epithelial cells were cultured in DMEM/F12 supplemented with B27 (Life technologies, Grand Island, NY), 10 mM of HEPES, Glutamax (Life technologies, Grand Island, NY), Penicillin/Streptomycin, and the following growth factors: EGF 50 ng/ml (Peprotech, Rocky Hill, NJ), 500 ng/ml of recombinant R-spondin1 (Peprotech, Rocky Hill, NJ), 100 ng/ml of recombinant Noggin (Peprotech, Rocky Hill, NJ), 200 μM of TGF-β/Alk inhibitor A83-01 (Tocris, Ellisville, MO), and 10 μM Y-27632 (Tocris, Ellisville, MO). Dihydrotestosterone (Sigma, St. Louis, MO) was added at 1 nM final concentration. 1–2 × 10^3 dissociated prostate cells were mixed with growth factor reduced matrigel (Corning, Corning, NY) by 1:1 ratio and plated in 96-well plates.

2.6. Cloning and generation of CD133 lentivirus

The cDNA encoding human CD133 was obtained from Dr. Donald Vander Griend at the University of Chicago. The cDNA was PCR amplified, verified by sequencing and cloned into the FU-CRW lentiviral vector using NheI (Xin et al., 2006). The primer sequences for human CD133 are (forward) 5′-CTAGCTAGCGCCACCATGGCCCTCGTACTCGGCT CC-3′ and (reverse) 5′-TGGGCTAGCTCACTTGTCGTCATCGTCTTTGTAG TCTCAATGTTGTGATGGGCTTG-3′. Lentivirus preparation and tittering were performed as described previously (Xin et al., 2003).

2.7. FACS

For the separation of prostate cell lineages, dissociated murine prostate cells were stained with Pacific blue-anti CD31, CD45 and Ter119 antibodies (eBioscience, San Diego, CA), PE-anti Sca-1 antibody (eBioscience, San Diego, CA), Alexa 647-anti CD49f antibody (Biolegend, San Diego, CA). PE-anti CD133 clone 13A4 (eBioscience, San Diego, CA) and clone 315-2C11 (Biolegend, San Diego, CA) were used to detect CD133. FACS analyses and sorting were performed by using the BD LSR II and Aria I, respectively (BD Biosciences, San Jose, CA).

2.8. RNA isolation and qRT-PCR

Total RNA was isolated from cells using the RNeasy Plus mini kit (Qiagen, Valencia, CA). Reverse transcription was performed using the iScript cDNA synthesis kit (Bio-Rad). qPCR was performed using the SYBR Premix Ex Taq (Perfect Real Time; Takara Bio Inc., Otsu, Shiga, Japan) on a StepOne plus Real-Time PCR system (Applied Biosystems,

Foster City, CA). qPCR primer sequences for CD133 are (forward) 5′-TTGGTGCAAATGTGGAAAAG-3′ and (reverse) 5′-ATTGCCATTGTTCCTTGAGC-3′.

2.9. Cytospin and staining

20,000–50,000 FACS-sorted cells were suspended in 200 μl 1 × PBS and cytospun onto glass slides using Cytology Funnel and Cytospin4 (Shandon, Thermo Scientific). Cells were fixed with 10% buffered formalin for 10 min at room temperature, and stained using standard immunocytochemistry techniques.

2.10. Immunostaining

Immunofluorescence staining were performed using standard protocols on 5-μm paraffin sections. Primary antibodies and dilutions used are listed in the Supplementary Table 2. Slides were incubated with 3% normal goat serum (Vector Labs) and with primary antibodies diluted in 3% normal goat serum overnight at 4 °C. Slides then were incubated with secondary antibodies (diluted 1:500 in 0.05% Tween 20 in phosphate-buffered saline (PBST)) labeled with Alexa Fluor 488 or 594 (Invitrogen/Molecular Probes). Sections were counterstained with 4,6-diamidino2-phenylindole (DAPI) (Sigma-Aldrich). Immunofluorescence staining was imaged using an Olympus BX60 fluorescence microscope or a Leica EL6000 confocal microscope. Images of IHC were analyzed by Image-Pro Plus version 6.3 by Media Cybernetics. Cell number was determined by using the count feature in the software that asks for the user to indicate the color that would be used to indicate a positive cell. (For example: blue would be indicated to count nuclei and thus indicate total numbers of cells). Borders were created such that only epithelial cells would be analyzed.

2.11. Western blot

Prostate tissues were lysed by using Tissuelyser LT (Qiagen) in RIPA buffer (20 mM Tris–HCl, pH 7.5, 150 mM NaCl, 1 mM Na_2EDTA, 1 mM EGTA, 1% NP-40, 1% sodium deoxycholate, 2.5 mM sodium pyrophosphate, 1 mM β-glycerophosphate and 1 mM Na_3VO_4) with protease inhibitors and phosphatase inhibitors (Roche Applied Science). Protein concentrations were determined by a Bradford Assay kit (Bio-Rad). Protein was separated by 10% SDS/PAGE and transferred onto a polyvinylidene difluoride (PVDF) membrane (Amersham Biosciences, Arlington Heights, IL). The membrane was blocked in 5% skim milk, and subsequently incubated with primary antibodies listed in Supplementary Table 2 at 4 °C overnight followed by incubation with peroxidase-conjugated goat anti-mouse IgG or goat anti-rabbit IgG (Jackson ImmunoResearch, Inc., West Grove, PA), and developed with Pierce ECL reagent (Thermo Scientific, Rockford, IL).

2.12. Statistical analysis

Slope scale was analyzed through linear repression with a 95% confidence interval. Statistical significance and the correlation coefficient (Pearson's r) were calculated using the correlation analysis. All the other statistical analyses were Student's t-test.

3. Results

3.1. The CD133-CreER^{T2} model labels CD133-expressing cells specifically

Previously, Zhu et al. generated a CD133-CreER^{T2} mouse model, in which the CreER^{T2} transgene was inserted downstream of the translational start site of the endogenous CD133 gene (Zhu et al., 2009). We sought to employ a lineage tracing approach using this mouse model to investigate whether CD133-expressing cells represent stem/progenitor cells in adult murine prostate epithelia. We bred the CD133-CreER^{T2} model with a Rosa26-eYFP reporter model that enables the expression of eYFP (enhanced yellow fluorescent protein) upon Cre-LoxP mediated homologous recombination and generated CD133-CreERT2$^{Wt/Mut}$-eYFP$^{Wt/Mut}$ mice (hereafter referred to as CD133-eYFP). CD133-eYFP mice still retain an intact CD133 allele and express a comparable level of CD133 to that of the wild type mice (Fig. S1A). When adult CD133-eYFP mice are treated with tamoxifen (Tmx), eYFP should be turned on in CD133-expressing cells.

CD133-CreER^{T2} model has been successfully employed to specifically label CD133-expressing cells in the small intestine and the skin (Snippert et al., 2009; Lin et al., 2014). To further validate the specificity of eYFP labeling in this model, RNA fluorescence *in situ* hybridization assay (FISH) was conducted to examine the localization of CD133 and eYFP mRNA. Because CD133 is expressed at a relatively higher level in the kidney, we performed FISH analysis using kidney tissues to facilitate signal detection. Briefly, 10-week-old CD133-eYFP mice were treated with tamoxifen for four consecutive days and the kidney tissues were harvested a day after the last tamoxifen treatment. Fig. 1A shows that eYFP mRNAs were generally detected in cells that expressed CD133 transcripts. To further validate the specificity of eYFP expression in CD133-expressing cells, we performed flow cytometric analyses to determine whether CD133 and eYFP proteins colocalize in individual cells. Fig. 1B and C show that 3.5% and 20% of the cells were eYFP$^+$/CD133$^+$ and eYFP$^-$/CD133$^+$, respectively. Unexpectedly, about 7% of the cells were eYFP$^+$/CD133$^-$, which was confirmed by FACS analyses using two different CD133 antibodies (Fig. 1B-C). However, qRT-PCR analysis revealed that eYFP$^+$/CD133$^-$ cells expressed a comparable level of CD133 with eYFP$^-$/CD133$^+$ and eYFP$^+$/CD133$^+$ cells (Fig. 1D). These eYFP$^+$/CD133$^-$ cells may be the newly born CD133$^+$ cells that have not been able to generate detectable levels of the CD133 protein. Alternatively, the enzymatic dissociation of murine prostate epithelial cells may negatively impact the expression or integrity of CD133 and diminish the recognition of CD133 by the antibodies in the FACS analysis. To test this hypothesis, we treated 293T cells expressing ectopic CD133 with the same enzymatic digestion protocol and determined how it affected CD133 expression by Western blot. Fig. 1E confirms that enzymatic digestion led to a reduction of CD133 protein level. Collectively, our study highlights a potential caveat of using antibodies to identify CD133-expressing cells and confirms CD133-eYFP as a valid model to label CD133-expressing cells.

3.2. CD133$^+$ cells are localized in basal, luminal and stromal compartments of murine prostate

We performed flow cytometric analyses to determine the identity of CD133-expressing cells in the prostate. Briefly, as shown in Fig. 2A, immediately after a four-day Tmx treatment, experimental mice were euthanized and prostate tissues were dissociated into single cells for FACS analysis. Basal cells (Lin$^-$/CD49f^{hi}/Sca-1$^+$), luminal cells (Lin$^-$/CD49f^{low}/Sca-1$^-$), and stromal cells (Lin$^-$/CD49f^{low}/Sca-1$^+$) were separated based on their surface antigenic expression profiles, as shown previously (Lawson et al., 2007). Fig. 2B shows the existence of CD133$^+$ cells in all three lineages (3.8%, 10% and 6.8% in basal cells, luminal cells, and stromal cells, respectively). Co-immunostaining analysis further corroborated the presence of eYFP$^+$ cells that expressed the basal cell markers Keratin 5 (K5) and P63, the luminal cell marker Keratin 8 (K8), and the stromal cell marker Smooth Muscle Actin (SMA), respectively (Fig. 2C). Collectively, these data demonstrate that CD133-expressing cells are present in all major prostate cell lineages.

3.3. Loss of function of CD133 does not impair the regenerative potential of prostate epithelia

Prostate epithelial cells atrophy and regenerate in response to alternating androgen ablation and replacement, which suggests the existence of stem cells with extensive regenerative capacity. The CD133-CreER^{T2} model was created so that the expression of the

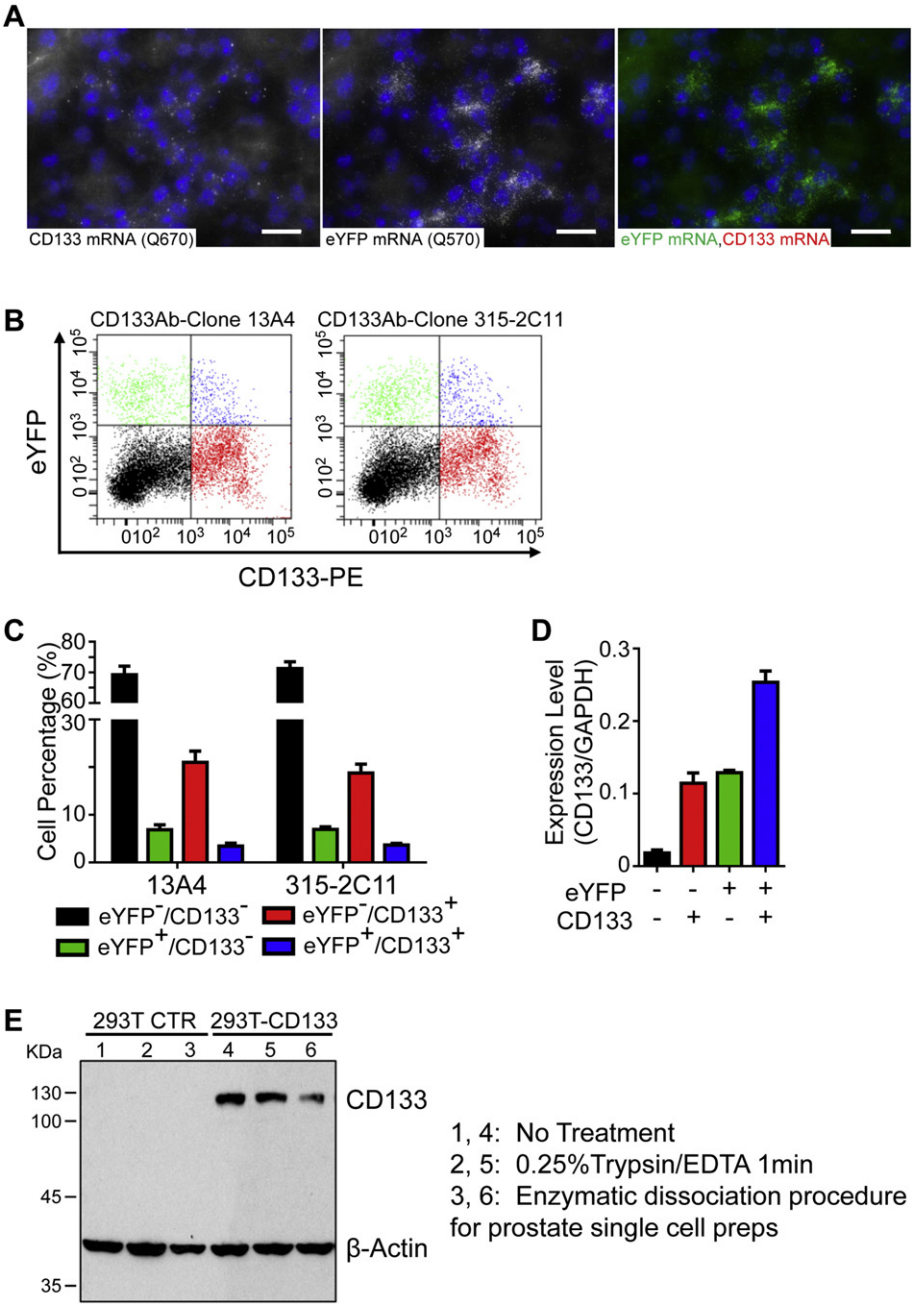

Fig. 1. The CD133-CreER^{T2} model labels CD133-expressing cells specifically. (A) RNA fluorescence *in situ* hybridization analysis of CD133 and eYFP in kidney tissues of tamoxifen-treated 10-week-old CD133-eYFP mice. Bars = 20 μm. (B) FACS plots of CD133 and eYFP in tamoxifen-treated CD133-eYFP mouse prostates. 13A4 and 315-2C11 are two different clones of CD133 antibodies. (C) Bar graph shows percentage of cell staining in FACS plots shown in Fig. 1B. Data represent means ± s.d. from three experimental mice. (D) qRT-PCR analysis of CD133 in the four FACS-sorted cell fractions. Data represent means ± s.d. from two independent experiments. (E) Western blot analysis of CD133 in CD133-expressing 293T cells with and without enzymatic treatment.

endogenous CD133 is replaced by the CreER^{T2} transgene, leading to a loss of function of CD133. We confirmed loss of expression of CD133 in CD133-CreER^{T2} homozygous mice by qRT-PCR, Western blot and flow cytometric analyses (Fig. S1). As shown in Fig. 3A, we conducted two cycles of androgen deprivation and replacement using control wild-type C57BL/6 mice and CD133 knockout (KO) mice, and determined whether loss of function of CD133 impairs the regenerative potential of prostate epithelial cells. Fig. 3B shows that the prostates of CD133 KO mice regressed and regenerated at the same dynamics as those of control mice. Therefore, CD133 knockout does not impair the regenerative capacity of murine prostate.

A prostate sphere assay was employed to further determine whether CD133 is crucial for the prostate stem cell activity. In this assay, dissociated prostate epithelial cells are cultured inside Matrigel in suspension. Only the putative stem cells in the basal cell lineage are able to form serially passagable spheroids (Xin et al., 2007). Dissociated prostate cells from wild type and CD133 KO mice were cultured in the sphere assay. Fig. 3C shows that CD133 KO cells displayed the same sphere-forming capacity with wild type cells. Loss of function of CD133 does not affect sphere cell self-renewal because KO spheres were capable of replating at similar frequencies as wild type prostate spheres (Fig. 3D). In addition, the sizes of the spheres generated from these two groups were comparable, suggesting that the wild type and CD133 KO cells proliferated at the same rate (Fig. 3C-D). Collectively, these data demonstrate that CD133 is functionally dispensable for the prostate stem cell activity.

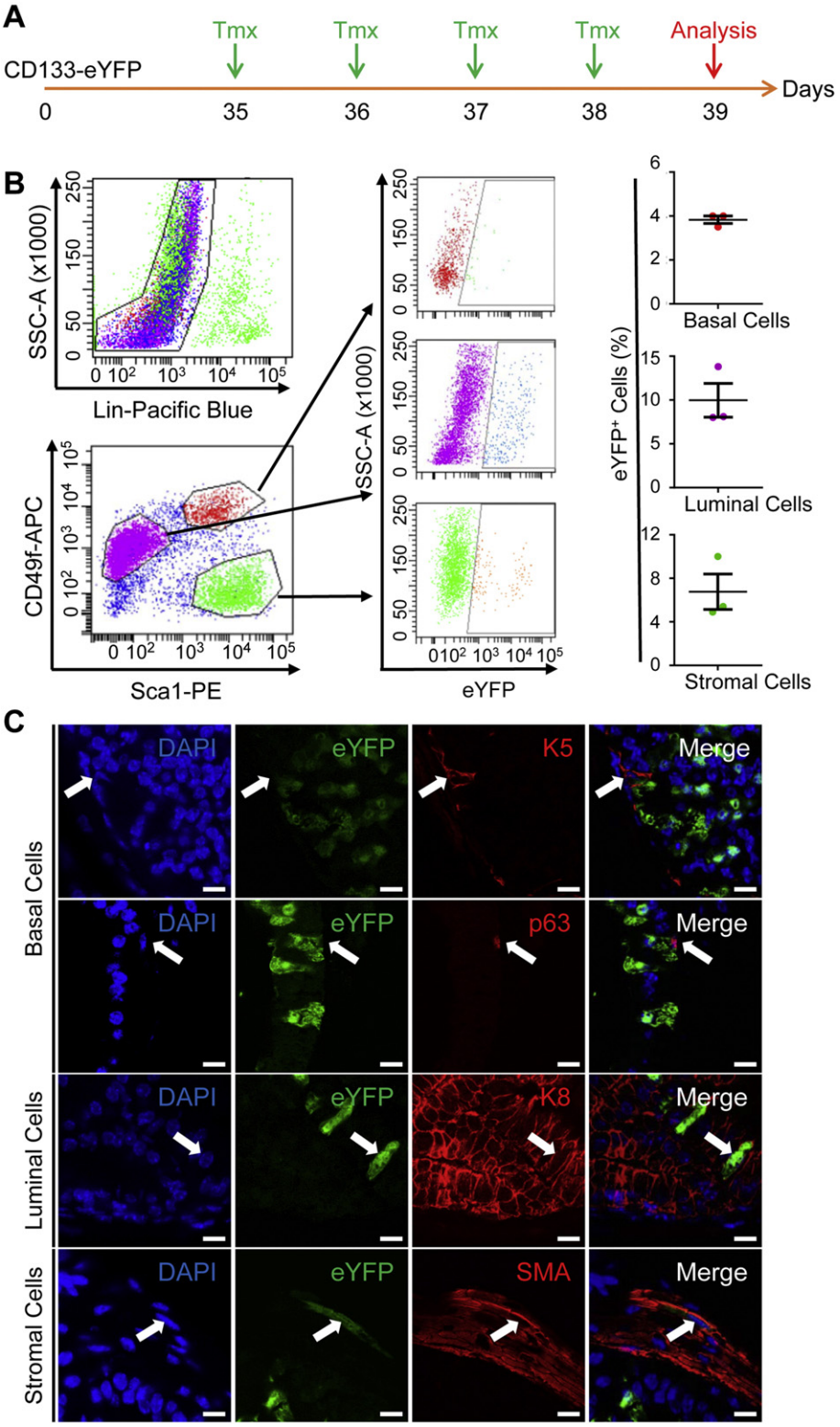

Fig. 2. CD133$^+$ cells are localized in basal, luminal and stromal compartments of murine prostate. (A) Schematic illustration of experimental design. Tmx: tamoxifen. (B) FACS plots of eYFP-expressing cells in basal, luminal and stromal cells. Dot graphs show means ± s.d. of percentage of eYFP-expressing cells in individual cell lineages from three independent experiments. (C) Coimmunostaining of eYFP with prostate lineage markers Keratin 5 (K5), P63, Keratin 8 (K8), and Smooth Muscle Actin (SMA), respectively. Arrows point to double-positive cells. Bars = 10 μm.

3.4. CD133$^+$ basal cells exhibit distinct stem cell potential in the prostate sphere assay and the prostate organoid assay

Previously, CD133 was shown to enrich for the clonogenic activity in human basal epithelial cells (Richardson et al., 2004). We sought to determine whether murine CD133$^+$ basal cells behave distinctly from CD133$^-$ basal cells in *in vitro* prostate stem cell assays. FACS-isolated eYFP$^+$ and eYFP$^-$ basal cells (Fig. 4A) were cultured in the prostate sphere assay (Xin et al., 2007) and a prostate organoid assay (Karthaus et al., 2014). Post-sorting immunofluorescence analysis

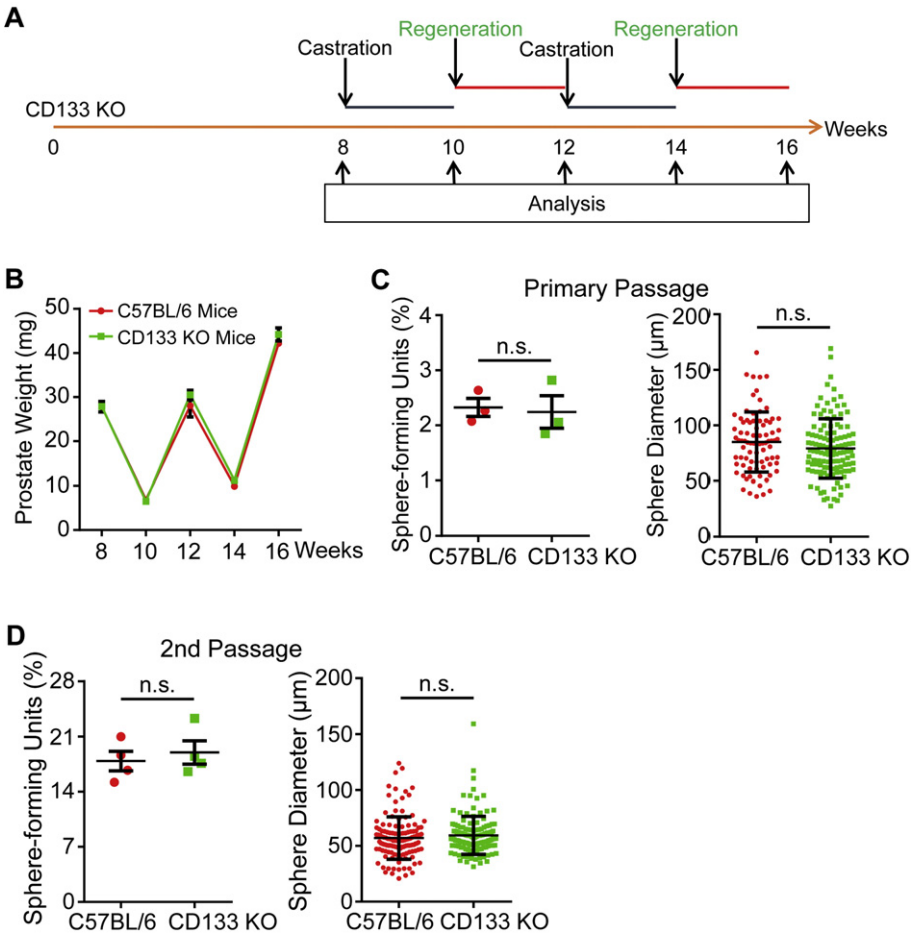

Fig. 3. CD133 is dispensable for the regenerative potential of prostate epithelia. (A) Schematic illustration of experimental design. Tmx: tamoxifen. (B) Dot graph shows means ± s.d. of prostatic weights of C57BL/6 control mice and CD133 knockout (KO) mice (n = 3 each) measured at the time points shown in Fig. 3A. (C) Dot graphs quantify sphere-forming units and sphere sizes in primary prostate sphere cultures from control and CD133 KO mouse prostate cells. Data represent means ± s.d. from three experimental mice. (D) Dot graphs quantify sphere-forming units and sphere sizes in secondary passage of prostate spheres derived from control and CD133 KO mouse prostate cells. Data represent means ± s.d. from three independent experiments.

confirms efficient cell separation (Fig. S2). Fig. 4B shows that the sphere-forming activity of eYFP$^+$ basal cells was approximately two-fold that of the eYFP$^-$ basal cells. In contrast, eYFP$^+$ basal cells formed organoids at the same frequency as eYFP$^-$ basal cells (Fig. 4D). No significant differences in size were detected between spheres or organoids generated by eYFP$^+$ and eYFP$^-$ basal cells (Fig. 4C, E), suggesting that these cells proliferated at the same rate.

Karthaus et al. showed that a small fraction of luminal cells were capable of forming organoids in the prostate organoid assay. To determine whether CD133 enriches for the luminal progenitor activity, we also compared the organoid-forming activities between FACS-isolated eYFP$^+$ and eYFP$^-$ luminal cells. Fig. 4F-G show that there were no significant differences in organoid-forming units or organoid sizes between the two groups, suggesting that CD133 does not enrich for the luminal progenitor activity.

3.5. CD133$^+$ and CD133$^-$ epithelial cells contribute equally to prostate epithelial maintenance and regeneration in vivo

We employed a lineage tracing assay to further investigate whether CD133-expressing cells may serve as the stem/progenitor cells *in vivo*. As shown in Fig. 5A, we labeled CD133-expressing cells in 8-week-old mice with eYFP and determined how these cells contribute to prostate epithelial homeostasis during aging. It should be noted that it is critical to wait for 10–14 days after tamoxifen treatment to allow the remaining tamoxifen to be completed metabolized before determining the percentage of eYFP-labeled cells accurately (Fig. 5A). Flow cytometric analysis revealed that the percentages of eYFP$^+$ cells in basal, luminal, and stromal cell compartments remained the same 28 weeks after Tmx treatment (Fig. 5B), suggesting that CD133-expressing cells are not functionally distinct from CD133$^-$ cells. Because prostate epithelial cells turn over infrequently under physiological conditions, we induced extensive epithelial cell turnover *via* two cycles of androgen deprivation and replacement and then determined the percentage of eYFP$^+$ cells by flow cytometric analysis (Fig. 5C). Fig. 5D shows that the percentages of eYFP$^+$ cells did not change significantly after induced epithelial cell turnover in all prostatic lobes. In addition, the ratios of eYFP$^+$ cells in prostate basal, luminal and stromal cells all remained constant (Fig. 5E). Collectively, these results demonstrate that CD133$^+$ and CD133$^-$ cells are functionally indistinguishable *in vivo* in adult murine prostate.

A complementary approach was employed to further investigate whether CD133$^+$ and CD133$^-$ cells contribute to epithelial regeneration equally. Briefly, as shown in Fig. 6A, we treated castrated mice with Tmx to label CD133-expressing cells and then replaced androgen to induce prostate regeneration. The proliferating indices of eYFP$^+$ and eYFP$^-$ cells were compared by Ki67 staining (Fig. 6B). If CD133-expressing cells contribute more to prostate regeneration, they should proliferate more frequently than CD133 negative cells. However, the percentage of proliferating CD133$^+$ cells (eYFP$^+$/Ki67$^+$%) correlated with that of the CD133-expressing cells in total cell population (eYFP$^+$%), corroborating that CD133-expressing cells are no better

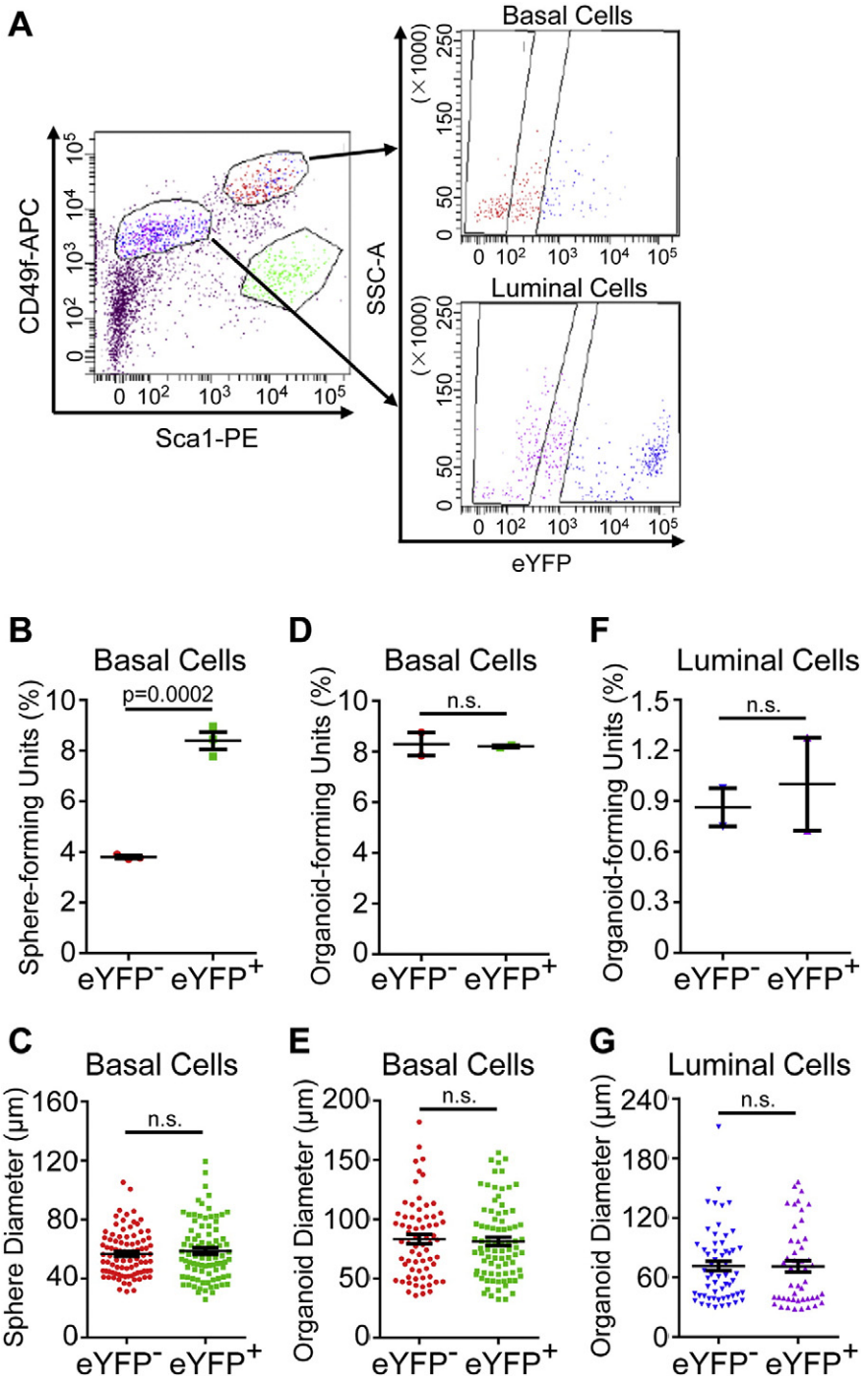

Fig. 4. CD133$^+$ basal cells exhibit distinct potential in the two different *in vitro* stem cell assays. (A) FACS plots of eYFP$^+$ cells in basal and luminal lineages in tamoxifen-treated CD133-eYFP mice. (B–C) Dot graphs quantify sphere-forming units and sphere sizes of eYFP$^+$ and eYFP$^-$ basal cells. Data show means ± s.d. from three independent experiments. (D–E) Dot graphs quantify organoid-forming units and organoid sizes of eYFP$^+$ and eYFP$^-$ basal cells. Data show means ± s.d. from two independent experiments. (F–G) Dot graphs quantify organoid-forming units and organoid sizes of eYFP$^+$ and eYFP$^-$ luminal cells. Data show means ± s.d. from two independent experiments.

than CD133 negative cells in responding to androgen-mediated growth stimuli (Fig. 6B and C).

4. Discussion

We investigated whether CD133 serves as a putative epithelial stem/progenitor cell marker in adult murine prostates and explored its function in prostate regenerative capacity. We demonstrated that CD133 is not only expressed in a small fraction of prostate basal cells but is also expressed in some luminal and stromal cells. Moreover, we compared the stem cell potential of CD133-expressing cells and their negative counterparts using both *in vitro* and *in vivo* approaches. Consistent with a previous study in human prostates (Richardson et al., 2004), we showed that murine CD133-expressing basal cells exhibited higher stem cell potential in the *in vitro* prostate sphere assay. However, lineage tracing analysis demonstrated an equal contribution of CD133-expressing cells and their negative counterparts to the maintenance of prostate epithelia. These observations are not necessarily in contradictory with each other because the experimental conditions are distinct in these assays. Instead, these results highlight that cell

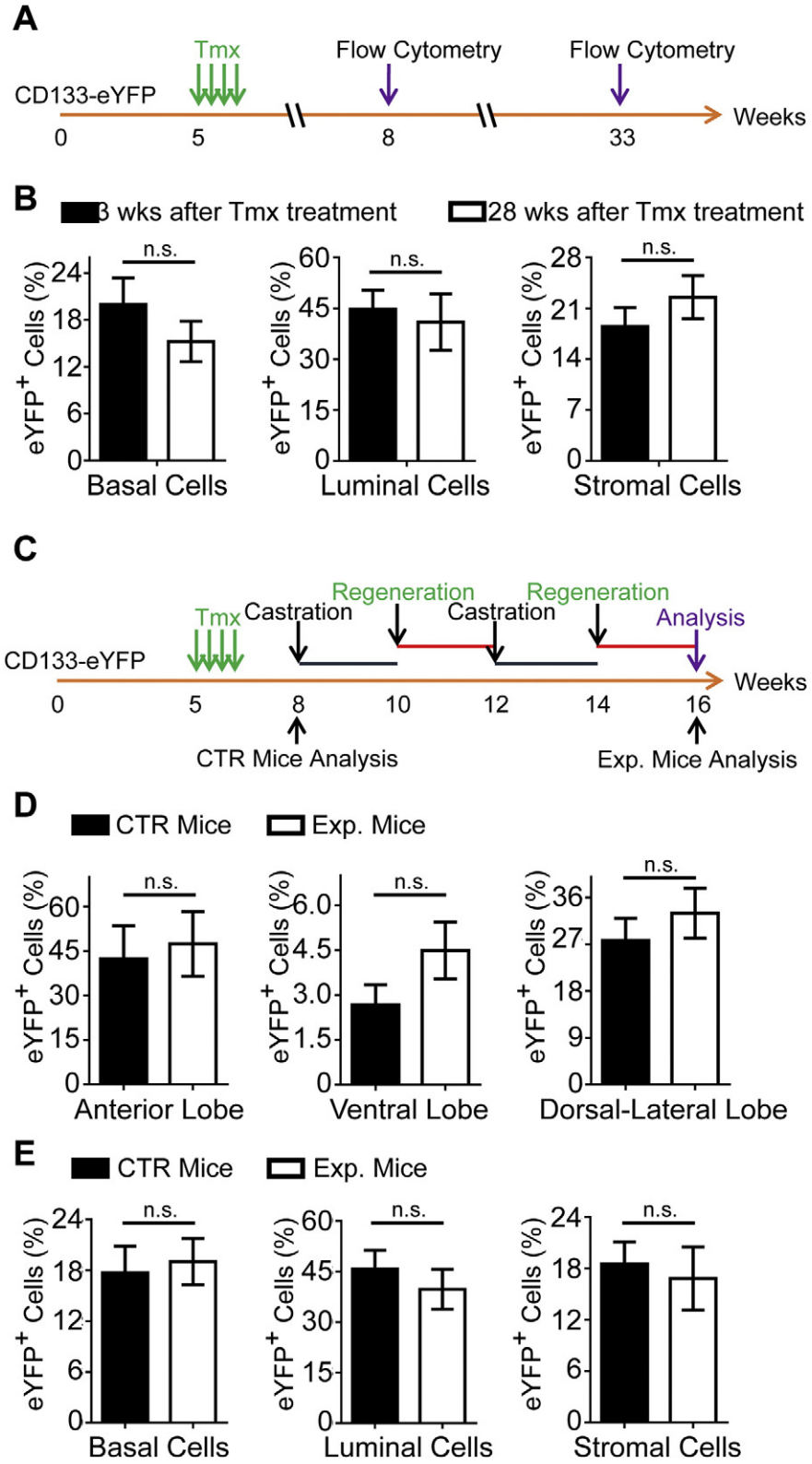

Fig. 5. CD133$^+$ and CD133$^-$ epithelial cells contribute equally to prostate epithelial maintenance and regeneration *in vivo*. (A) Schematic illustration of the lineage tracing experiment during aging. Tmx: tamoxifen. (B) Bar graphs show percentages of eYFP$^+$ cells in basal cells, luminal cells, and stromal cells at 3 weeks and 28 weeks after Tmx treatment. Data show means ± s.d. from 8 and 4 mice for 3 weeks and 28 weeks after Tmx treatment, respectively. (C) Schematic illustration of the lineage tracing experiment during prostate regeneration. (D) Bar graphs show percentages of eYFP$^+$ cells in anterior, ventral, and dorsal-lateral lobes of tamoxifen-treated CD133-eYFP mice before (Ctr) and after (Exp) two cycles of androgen deprivation and replacement. Data show means ± s.d. from 12 and 11 mice for Ctr and Exp groups, respectively. (E) Bar graphs show percentages of eYFP$^+$ cells in prostate basal, luminal, and stromal cells of tamoxifen-treated CD133-eYFP mice before (Ctr) and after (Exp) two cycles of androgen deprivation and replacement. Data show means ± s.d. from 8 and 7 mice for Ctr and Exp groups, respectively.

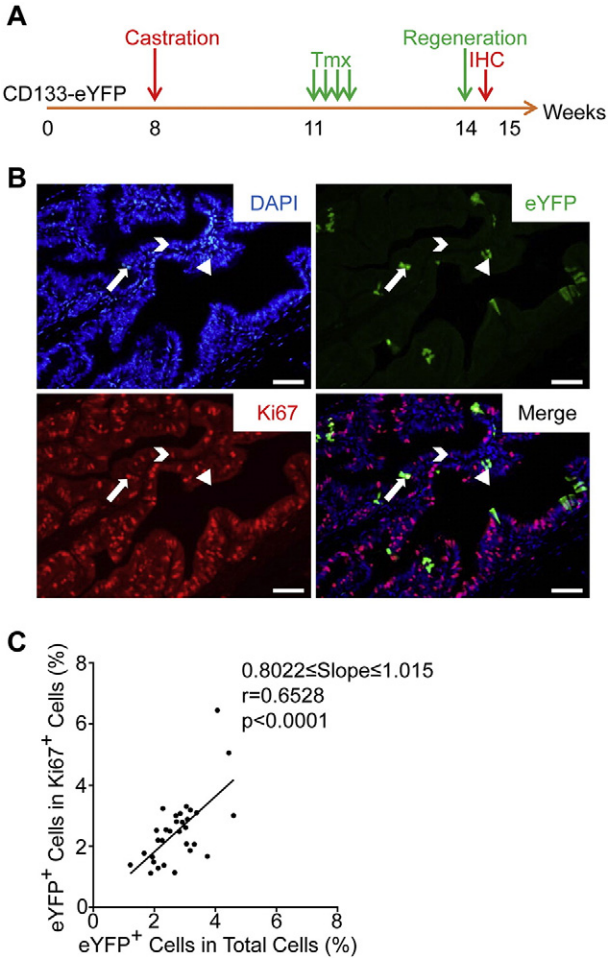

Fig. 6. CD133$^+$ and CD133$^-$ cells possess the same proliferative capacity during induced prostate regeneration. (A) Schematic illustration of experimental design. Tmx: tamoxifen. (B) Immunofluorescence analysis of eYFP and Ki67 in prostates of tamoxifen-treated CD133-eYFP mice after androgen deprivation and replacement. Notched-arrows, arrowheads, and arrows point to eYFP$^-$Ki67$^+$, eYFP$^+$Ki67$^-$, and eYFP$^+$Ki67$^+$ cells, respectively. Bars = 50 μm. (C) Dot graph shows statistical correlation between percentage of newly-formed eYFP$^+$ cells (eYFP$^+$ cells in Ki67$^+$ cells) and percentage of eYFP labeling (eYFP$^+$ cells in total cells). Data represent quantification of 31 images from four experimental mice.

behaviors can be determined by their biological contexts. Because the experimental condition in the lineage tracing approach is more physiologically relevant, we believe that CD133 does not enrich for the prostate stem cell activities *in vivo*. Finally, we also demonstrated that CD133 is functionally dispensable for prostate epithelial homeostasis and regeneration under the experimental contexts in this study. Of course, we cannot rule out that loss of CD133 may affect specific cell behaviors in other biological contexts not tested in our study.

To this end, it remains unknown why CD133-expressing cells behave distinctly in different stem cell assays. One potential explanation is that the available signaling for cell survival and proliferation is different in these assays. The prostate sphere culture contains a minimal of growth factors such as EGF and FGF, and provides very basic cell signaling that support cell survival and proliferation. CD133 has been shown to potentiate activation of the PI3K/Akt pathway by directly interacting with the p85 subunit of PI3K and promoting phosphorylation of Akt (Wei et al., 2013). Pharmacological inhibition of the PI3K activity in the prostate cancer cell lines DU145 and PC3 decreased the percentage of the CD133$^+$/CD44$^+$ prostate cancer stem cells as well as their sphere-forming activity (Dubrovska et al., 2009). Therefore, CD133-expressing basal cells may have a relatively higher basal level of PI3K-Akt activity, which confers a minor survival advantage on them in the prostate sphere assay. In contrast, additional signaling regulating cell survival, differentiation and proliferation are provided in the organoid assay, such as augmentation of the Wnt signaling and suppression of the TGFβ signaling. These signaling have been shown to suppress apoptosis and anoikis (Yang et al., 2006; Orford et al., 1999; Chen et al., 2001; Ramachandra et al., 2002; Cao et al., 2006). They may override CD133-mediated signaling in the organoid assay and mask the minor survival advantage mediated by CD133. Similarly, in the *in vivo* lineage tracing assay, the challenge for cell survival does not serve as a prerequisite for assaying stem cell activity, thereby revealing the equal potential of the CD133$^+$ and CD133$^-$ cells in maintaining epithelial homeostasis and regeneration. Collectively, our study corroborates that facultative function of specific cell populations induced by experimental conditions may not contribute to the *in vivo* biology substantially.

Although our study shows that CD133$^+$ cells and CD133$^-$ cells behave similarly *in vivo* in maintaining epithelial homeostasis and regeneration, CD133$^+$ and CD133$^-$ cells have been shown to play distinct roles in prostate cancer initiation. Taylor RA et al. showed that CD133$^-$ cells in an immortalized BPH-1 human prostate epithelial cell line are more proliferative and more susceptible to transformation induced by cancer-associated fibroblasts or hormonal stimulation (Taylor et al., 2012). In addition, CD133$^+$ and CD133$^-$ cells are also shown to be functionally distinct in several tumor studies. For example, CD133$^+$ cells in human prostate cancer cell lines proliferated faster *in vitro* (Reyes et al., 2013) and CD133$^+$ cells in human prostate cancer specimens possessed cancer stem cell activity (Vander Griend et al., 2008; Collins et al., 2005). It remains an open question whether CD133-mediated signaling dictates the functional outcome in these studies, or these studies imply that CD133 expression and putative cancer stem cell activity are co-regulated by the same signaling. Future studies using mouse models for prostate cancer should help address this question.

Supplementary data to this article can be found online at http://dx.doi.org/10.1016/j.scr.2016.03.003.

Author contribution

X.W. and L.X. designed the experiments.
X.W. and A.V.O. performed experiments and acquired data.
X.W and L.X. analyzed the data and wrote the manuscript.

Acknowledgment

We thank Dr. Donald Vander Griend for providing CD133 cDNA, Dr. Oh-Joon Kwon and Ms. Li Zhang for technical help, the technical support by the Cytometry and Cell Sorting Core at Baylor College of Medicine with funding from the NIH (P30 AI036211, P30 CA125123, and S10 RR024574) and the expert assistance of Joel M. Sederstrom. This work is supported by NIH R01 DK092202 (L.X.) and NIH P30 CA125123 (the Cancer Center Shared Resources Grant).

References

Alessandri, G., et al., 2004. Isolation and culture of human muscle-derived stem cells able to differentiate into myogenic and neurogenic cell lineages. Lancet 364 (9448), 1872–1883.
Belicchi, M., et al., 2004. Human skin-derived stem cells migrate throughout forebrain and differentiate into astrocytes after injection into adult mouse brain. J. Neurosci. Res. 77 (4), 475–486.
Cao, Y., Deng, C., Townsend Jr., C.M., Ko, T.C., 2006. TGF-beta inhibits Akt-induced transformation in intestinal epithelial cells. Surgery 140 (2), 322–329.
Chen, S., et al., 2001. Wnt-1 signaling inhibits apoptosis by activating beta-catenin/T cell factor-mediated transcription. J. Cell Biol. 152 (1), 87–96.
Collins, A.T., Berry, P.A., Hyde, C., Stower, M.J., Maitland, N.J., 2005. Prospective identification of tumorigenic prostate cancer stem cells. Cancer Res. 65 (23), 10946–10951.
Dail, M., et al., 2014. Loss of oncogenic Notch1 with resistance to a PI3K inhibitor in T-cell leukaemia. Nature 513 (7519), 512–516.
Dubrovska, A., et al., 2009. The role of PTEN/Akt/PI3K signaling in the maintenance and viability of prostate cancer stem-like cell populations. Proc. Natl. Acad. Sci. U. S. A. 106 (1), 268–273.

Facciponte, J.G., et al., 2014. Tumor endothelial marker 1-specific DNA vaccination targets tumor vasculature. J. Clin. Invest. 124 (4), 1497–1511.
Florek, M., et al., 2005. Prominin-1/CD133, a neural and hematopoietic stem cell marker, is expressed in adult human differentiated cells and certain types of kidney cancer. Cell Tissue Res. 319 (1), 15–26.
Karbanova, J., et al., 2008. The stem cell marker CD133 (prominin-1) is expressed in various human glandular epithelia. J. Histochem. Cytochem. 56 (11), 977–993.
Karthaus, W.R., et al., 2014. Identification of multipotent luminal progenitor cells in human prostate organoid cultures. Cell 159 (1), 163–175.
Kordes, C., et al., 2007. CD133+ hepatic stellate cells are progenitor cells. Biochem. Biophys. Res. Commun. 352 (2), 410–417.
Kwon, O.J., Zhang, L., Xin, L., 2015. Stem cell antigen-1 identifies a distinct androgen-independent murine prostatic luminal cell lineage with bipotent potential. Stem Cells.
Lawson, D.A., Xin, L., Lukacs, R.U., Cheng, D., Witte, O.N., 2007. Isolation and functional characterization of murine prostate stem cells. Proc. Natl. Acad. Sci. U. S. A. 104 (1), 181–186.
Lin, Q., et al., 2014. Pharmacological mobilization of endogenous stem cells significantly promotes skin regeneration after full-thickness excision: the synergistic activity of AMD3100 and tacrolimus. J. Invest. Dermatol. 134 (9), 2458–2468.
Maw, M.A., et al., 2000. A frameshift mutation in prominin (mouse)-like 1 causes human retinal degeneration. Hum. Mol. Genet. 9 (1), 27–34.
Miraglia, S., et al., 1997. A novel five-transmembrane hematopoietic stem cell antigen: isolation, characterization, and molecular cloning. Blood 90 (12), 5013–5021.
Missol-Kolka, E., et al., 2011. Prominin-1 (CD133) is not restricted to stem cells located in the basal compartment of murine and human prostate. Prostate 71 (3), 254–267.
Orford, K., Orford, C.C., Byers, S.W., 1999. Exogenous expression of beta-catenin regulates contact inhibition, anchorage-independent growth, anoikis, and radiation-induced cell cycle arrest. J. Cell Biol. 146 (4), 855–868.
Oshima, Y., et al., 2007. Isolation of mouse pancreatic ductal progenitor cells expressing CD133 and c-met by flow cytometric cell sorting. Gastroenterology 132 (2), 720–732.
Ramachandra, M., et al., 2002. Restoration of transforming growth factor Beta signaling by functional expression of smad4 induces anoikis. Cancer Res. 62 (21), 6045–6051.
Reyes, E.E., Kunovac, S.K., Duggan, R., Kregel, S., Vander Griend, D.J., 2013. Growth kinetics of CD133-positive prostate cancer cells. Prostate 73 (7), 724–733.
Richardson, G.D., et al., 2004. CD133, a novel marker for human prostatic epithelial stem cells. J. Cell Sci. 117 (Pt 16), 3539–3545.
Shmelkov, S.V., et al., 2008. CD133 expression is not restricted to stem cells, and both CD133+ and CD133- metastatic colon cancer cells initiate tumors. J. Clin. Invest. 118 (6), 2111–2120.
Snippert, H.J., et al., 2009. Prominin-1/CD133 marks stem cells and early progenitors in mouse small intestine. Gastroenterology 136 (7), 2187–2194 e2181.
Taylor, R.A., et al., 2012. Human epithelial basal cells are cells of origin of prostate cancer, independent of CD133 status. Stem Cells 30 (6), 1087–1096.
Valdez, J.M., et al., 2012. Notch and TGFbeta form a reciprocal positive regulatory loop that suppresses murine prostate basal stem/progenitor cell activity. Cell Stem Cell 11 (5), 676–688.
Vander Griend, D.J., et al., 2008. The role of CD133 in normal human prostate stem cells and malignant cancer-initiating cells. Cancer Res. 68 (23), 9703–9711.
Wei, Y., et al., 2013. Activation of PI3K/Akt pathway by CD133-p85 interaction promotes tumorigenic capacity of glioma stem cells. Proc. Natl. Acad. Sci. U. S. A. 110 (17), 6829–6834.
Weigmann, A., Corbeil, D., Hellwig, A., Huttner, W.B., 1997. Prominin, a novel microvilli-specific polytopic membrane protein of the apical surface of epithelial cells, is targeted to plasmalemmal protrusions of non-epithelial cells. Proc. Natl. Acad. Sci. U. S. A. 94 (23), 12425–12430.
Xin, L., Ide, H., Kim, Y., Dubey, P., Witte, O.N., 2003. In vivo regeneration of murine prostate from dissociated cell populations of postnatal epithelia and urogenital sinus mesenchyme. Proc. Natl. Acad. Sci. U. S. A. 100 (Suppl. 1), 11896–11903.
Xin, L., et al., 2006. Progression of prostate cancer by synergy of AKT with genotropic and nongenotropic actions of the androgen receptor. Proc. Natl. Acad. Sci. U. S. A. 103 (20), 7789–7794.
Xin, L., Lukacs, R.U., Lawson, D.A., Cheng, D., Witte, O.N., 2007. Self-renewal and multilineage differentiation in vitro from murine prostate stem cells. Stem Cells 25 (11), 2760–2769.
Yang, F., Zeng, Q., Yu, G., Li, S., Wang, C.Y., 2006. Wnt/beta-catenin signaling inhibits death receptor-mediated apoptosis and promotes invasive growth of HNSCC. Cell. Signal. 18 (5), 679–687.
Yang, Z., et al., 2008. Mutant prominin 1 found in patients with macular degeneration disrupts photoreceptor disk morphogenesis in mice. J. Clin. Invest. 118 (8), 2908–2916.
Yin, A.H., et al., 1997. AC133, a novel marker for human hematopoietic stem and progenitor cells. Blood 90 (12), 5002–5012.
Zacchigna, S., et al., 2009. Loss of the cholesterol-binding protein prominin-1/CD133 causes disk dysmorphogenesis and photoreceptor degeneration. J. Neurosci. 29 (7), 2297–2308.
Zhang, Q., et al., 2007. Severe retinitis pigmentosa mapped to 4p15 and associated with a novel mutation in the PROM1 gene. Hum. Genet. 122 (3–4), 293–299.
Zhu, L., et al., 2009. Prominin 1 marks intestinal stem cells that are susceptible to neoplastic transformation. Nature 457 (7229), 603–607.